Supplementary material

Pathway and enzyme engineering for the bioconversion of lignin derivatives into homoeriodictyol in *Saccharomyces cerevisiae*

Si-Yu Zhu[a,b], Shi-Chang Liu[a,b], Chuan-Xi Zhang[c], Xin Xin[a,b], Zhi-Hua Liu[a,b], Lu-Jia Zhang[d,e], Bing-Zhi Li[a,b,*], Ying-Jin Yuan[a,b]

[a] Frontiers Science Center for Synthetic Biology and Key Laboratory of Systems Bioengineering (Ministry of Education), School of Chemical Engineering and Technology, Tianjin University, Tianjin 300072, China.

[b] Frontiers Research Institute for Synthetic Biology, Tianjin University, Tianjin 300072, China.

[c] Department of Micro/Nano Electronics, School of Electronic Information and Electrical Engineering, Shanghai Jiao Tong University, Shanghai 200240, China.

[d] Shanghai Engineering Research Center of Molecular Therapeutics New Drug Development, School of Chemistry and Molecular Engineering, East China Normal University, Shanghai 200062, China.

[e] NYU-ECNU Center for Computational Chemistry at NYU Shanghai, Shanghai 200062, China.

[*]Corresponding author.

E-mail address: bzli@tju.edu.cn (B. Li)

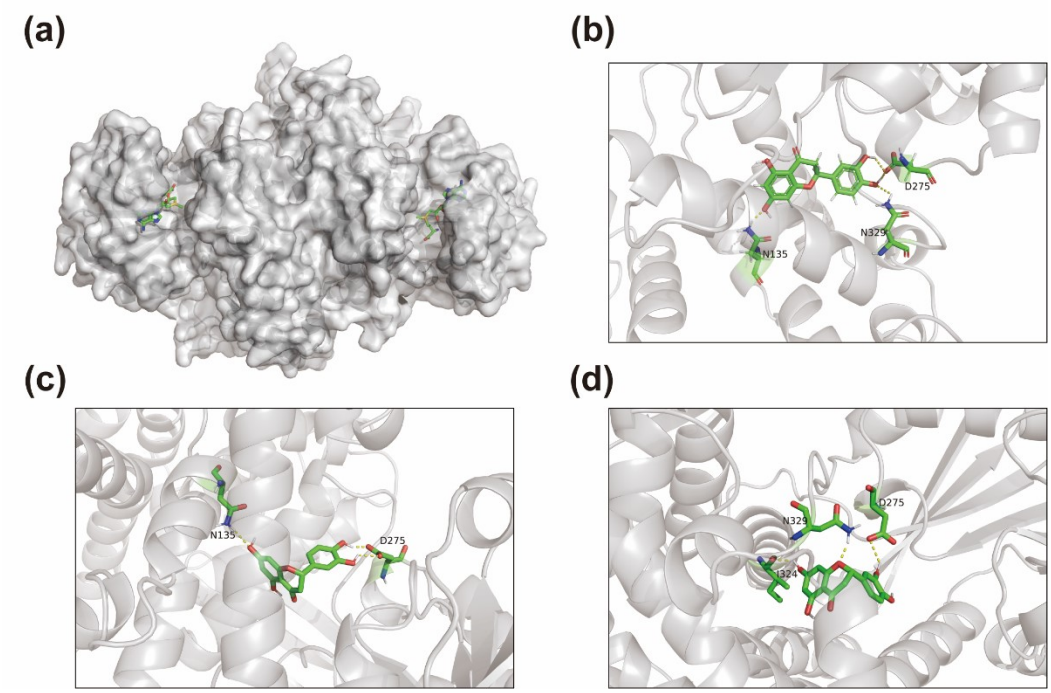

Fig. S1. Homology modeling of *Os*Romt-9 and docking results of *Os*Romt-9-eriodictyol. (a) Homology modeling of *Os*Romt-9 using Caffeic acid O-methyltransferase from *Sorghum bicolor* as template; (b, c, d) Reliable docking results of *Os*Romt-9 and eriodictyol. The yellow dashed lines indicate the hydrogen bonds between enzyme and substrate.

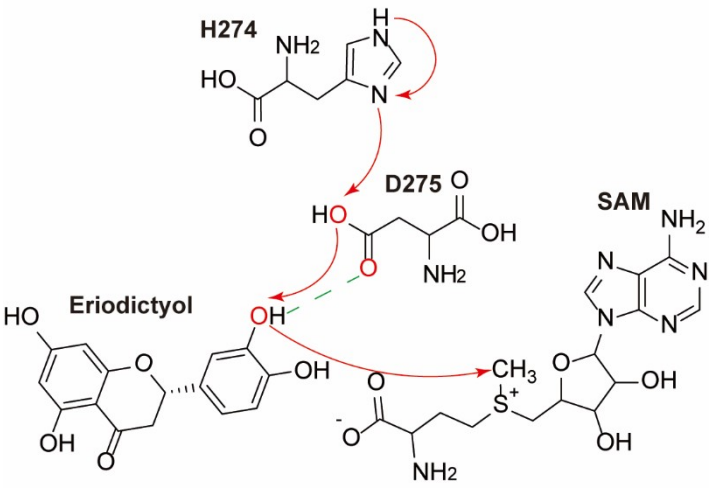

Fig. S2. Hypothetical mechanism of *Os*Romt-9. The electron is transferred from water molecules in the reaction center to the imidazole ring of His274, and then to Asp275, resulting in 3'-hydroxyl group becoming an electron-enriched group. Finally, the methyl group of SAM is nucleophilic attacked by 3'-hydroxyl group of eriodictyol to form homoeriodictyol and SAH.

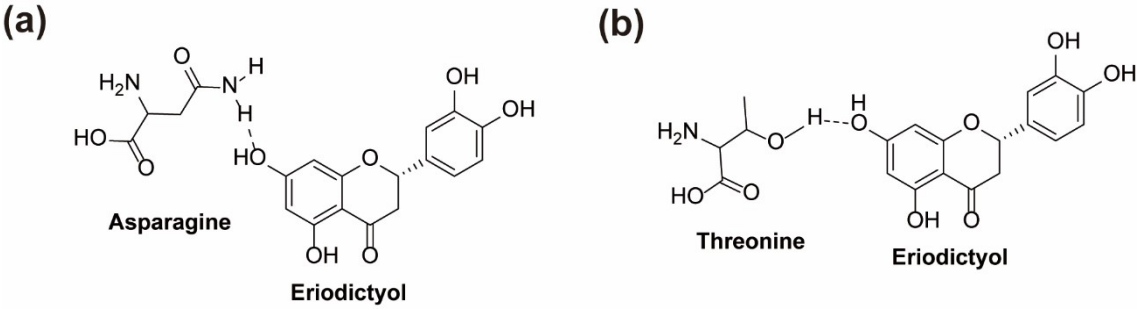

Fig. S3. The hydrogen bond formation of eriodictyol-*Os*Romt-9 and eriodictyol-*Os*Romt-9^{N135T}.

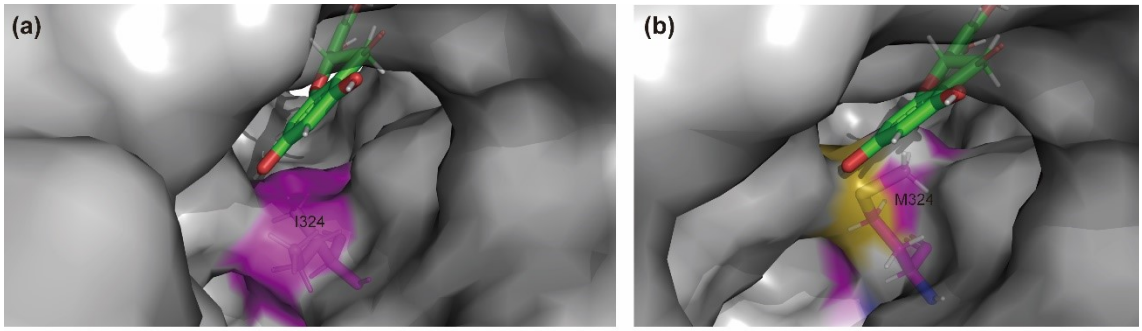

Fig. S4. The binding pocket of eriodictyol-*Os*Romt-9^{N135T} and eriodictyol-*Os*Romt-9$^{N135T/I324M}$. The I324M mutation changed the shape of the binding pocket, which made the substrate bound to the enzyme more tightly.

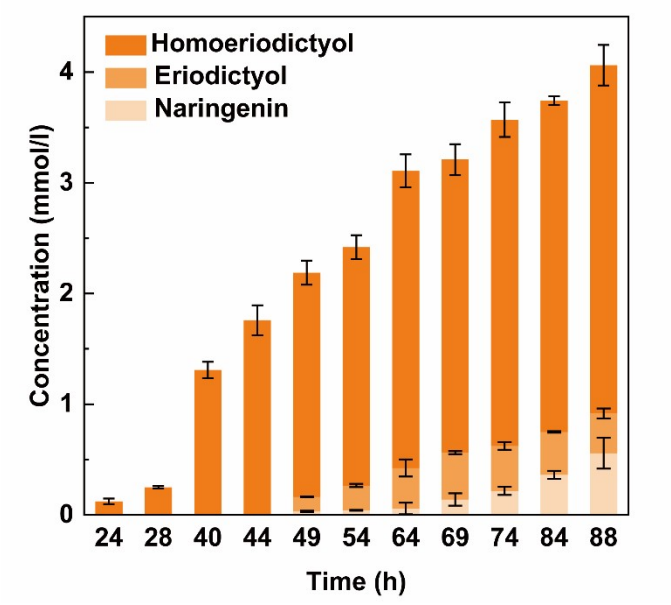

Fig. S5. The accumulation of intermediates and the production of homoeriodictyol during the fed-batch fermentation.

Table S1. List of plasmids constructed in this study

Strains	Description
pRS101	pRS413-P_{TEF1}-*ACS1*-T_{ADH1}
pRS102	pRS413-P_{TEF1}-*ACS2*-T_{ADH1}
pRS103	pRS413-P_{TEF1}-*Pc4CL*-T_{ADH1}
pRS104	pRS413-P_{TEF1}-*PhCHS*-T_{ADH1}
pRS105	pRS413-P_{TEF1}-*MsCHI*-T_{ADH1}
pRS106	pRS413-P_{TEF1}-*MsCHI-PhCHS*-T_{ADH1}
pRS107	pRS413-P_{TEF1}-*PhCHS-(GGGGS)1-MsCHI*-T_{ADH1}
pRS108	pRS413-P_{TEF1}-*PhCHS-(GGGGS)2-MsCHI*-T_{ADH1}
pRS109	pRS413-P_{TEF1}-*PhCHS-(GGGGS)3-MsCHI*-T_{ADH1}
pRS110	pRS413-P_{TEF1}-*MsCHI-(GGGGS)1-PhCHS*-T_{ADH1}
pRS111	pRS413-P_{TEF1}-*MsCHI-(GGGGS)2-PhCHS*-T_{ADH1}
pRS112	pRS413-P_{TEF1}-*MsCHI-(GGGGS)3-PhCHS*-T_{ADH1}
pRS113	pRS413- P_{GPM1}-*SAH1*-T_{TEF2}
pRS114	pRS413- P_{TEF1}-*ADO1*-T_{ADH1}
pRS115	pRS413- P_{TPI1}-*MET6*-T_{CPS1}
pRS116	pRS413- P_{TDH3}-*MET13-MTHFR*-T_{CYC1}

Table S2. List of strains constructed in this study

Strains	Description
Yzsy001	CEN.PK2-1D, *delta15*::P_{TPI1}-*Pc4CL*-T_{CPS1}-P_{GPM1}-*MsCHI*-T_{TEF2}-P_{TEF1}-*PhCHS*-T_{ADH1}
Yzsy002	Yzsy001, *delta22*::P_{GPM1}-*ATR1*-T_{TEF2}-P_{TEF1}-*AtF3'H*-T_{ADH1}
Yzsy003	Yzsy001, *delta22*::P_{GPM1}-*ATR1*-T_{TEF2}-P_{TEF1}-*AtF3'H*-T_{ADH1}-P_{TPI1}-*OsROMT-9*-T_{CPS1}
Yzsy004	Yzsy001, *delta22*::P_{GPM1}-*ATR1*-T_{TEF2}-P_{TEF1}-*AtF3'H*-T_{ADH1}-P_{TPI1}-*CrOMT2*-T_{CPS1}
Yzsy005	Yzsy001, *delta22*::P_{GPM1}-*ATR1*-T_{TEF2}-P_{TEF1}-*AtF3'H*-T_{ADH1}-P_{TPI1}-*VvFAOMT*-T_{CPS1}
Ynar001	CEN.PK2-1D, *delta15*::P_{TPI1}-*Pc4CL*-T_{CPS1}-P_{GPM1}-*MsCHI*-T_{TEF2}-P_{TEF1}-*PhCHS*-T_{ADH1}
Ynar002	Ynar001, ΔP_{ACC1}::P_{TEF1}
Ynar003	Ynar002, pRS101
Ynar004	Ynar002, pRS102
Ynar005	Ynar002, Δ*CIT2*
Ynar006	Ynar002, Δ*MLS1*
Ynar007	Ynar002, ΔP_{MLS1}::P_{CHO1}
Ynar008	Ynar005, Δ*FDC1*
Ynar009	Ynar008, Δ*PAD1*
Ynar010	Ynar008, Δ*TSC13*:: *MdECR*
Ynar011	Ynar010, pRS103
Ynar012	Ynar010, pRS104
Ynar013	Ynar010, pRS105
Ynar014	Ynar010, pRS106
Ynar015	Ynar010, pRS107
Ynar016	Ynar010, pRS108
Ynar017	Ynar010, pRS109
Ynar018	Ynar010, pRS110
Ynar019	Ynar010, pRS111
Ynar020	Ynar010, pRS112
Ynar021	Ynar010, *Ty3*::P_{TEF1}-*MsCHI*-*(GGGGS)1*-*PhCHS*-T_{ADH1}
Yeri001	Ynar021, *delta22*::P_{GPM1}-*ATR1*-T_{TEF2}-P_{TEF1}-*AtF3'H*-T_{ADH1}
Yher001	Yeri001, *Ty1*::P_{TPI1}-*OsROMT-9*-T_{CPS1}
Yher002	Yher001, pRS113
Yher003	Yher001, pRS114
Yher004	Yher001, pRS115
Yher005	Yher001, pRS116
Yher006	Yher001, *HO*:: P_{TPI1}-*MET6*-T_{CPS1}-P_{GPM1}-*SAH1*-T_{TEF2}-P_{TEF1}-*ADO1*-T_{ADH1}- P_{TDH3}-*MET13*-*MTHFR*-T_{CYC1}
Yher007	Yeri001, *HO*:: P_{TPI1}-*MET6*-T_{CPS1}-P_{GPM1}-*SAH1*-T_{TEF2}-P_{TEF1}-*ADO1*-T_{ADH1}- P_{TDH3}-*MET13*-*MTHFR*-T_{CYC1}, *Ty1*::P_{TPI1}-*OsROMT-9*$^{N135T/I324M}$-T_{CPS1}